Journal of Orthopaedic Surgery and Research

RESEARCH

Open Access

Tuina promotes nerve myelin regeneration in SNI rats through Piezo1/YAP/TAZ pathway

Yue Xu[1], Na Rentuya[1], Tianyuan Yu[1*], Jiawang Yan[1], Hongzheng Zhang[1], Yingqi Zhang[1], Hanyu Zhang[1], Jiawei Sun[1] and Jiayue Liu[1]

Abstract

Purpose The changes in the mechanical environment of local nerves after peripheral nerve injury (PNI) can cause a series of mechanical electrochemical signal reactions that affect the process of nerve regeneration and functional recovery. Piezo1/YAP/TAZ is an important transduction pathway that affects myelin regeneration. Our previous studies showed that Tuina could treat PNI in a variety of ways, including promoting nerve repair. However, whether Tuina as a kind of benign mechanical stimulation could promote nerve repair by changing the neuromechanical environment and causing changes in the mechanical electrochemical signal transduction pathway Piezo1/YAP/TAZ is unknown.

Methods The rats were divided into 4 groups, Sham group, sciatic nerve injury (SNI) group, Tuina group and Tuina + GsMTx4 group, with 6 rats in each group. We established an SNI model. Sciatic nerves at the mid-thigh level were exposed and crushed using a pair of non-serrated forceps for 5 s and the damage points about 2 mm. We used a Tuina manipulation emulator designed by our team to intervent. According to the "Three-Manipulation and Three-Acupoint": the emulator was used to perform the Dian, Bo, and Rou methods on Yinmen (BL37), Chengshan (BL57) and Yanglingquan (GB34) sequentially on the affected side. Each Tuina method was applied for 1 min on each acupoint respectively. Tuina treatment was administered once daily for 20 days. And we observed Somatic Functional Index (SFI), Mechanical Withdrawal Threshold (MWT), electrophysiological test and Shear wave elastography (SWE) examination in each group. Toluidine blue staining was performed to observe nerve fibers. The expression of Piezo1, Yes-associated protein (YAP), transcriptional coactivator with PDZ-binding motif (TAZ), Myelin basic protein (MBP), Neurofilament 200 (NF200), S100 calcium-binding protein β(S100β) and Ca^{2+} were detected using Immunofluorescence (IF), Western Blot (WB), Real-Time Quantitative PCR (RT-PCR) and Calcium Assay Kit.

Results Tuina improved the SFI, MWT, and compound action potential (CMAP) changes after SNI. The SWE results showed that Tuina reduced Emax and Smax. Piezo1, Ca^{2+} expression were reduced, YAP, TAZ, MBP, NF200, S100β expression were enhanced by Tuina.

Conclusion The activation of Schwann cells (SCs) and the regeneration of injured nerve myelin post-Tuina intervention are associated with alterations in the Piezo1/YAP/TAZ signaling pathway within SCs, induced by the mechanical forces generated through Tuina.

Keywords Tuina, Three-manipulation and three-acupoint, Piezo1, YAP, TAZ

*Correspondence:
Tianyuan Yu
yutianyuan@sina.com
[1]School of Acupuncture, Moxibustion and Tuina, Beijing University of Chinese Medicine, Beijing, People's Republic of China

Introduction

Peripheral nerve injury (PNI) is a prevalent condition in clinical practice and constitutes a significant contributor to substantial social and economic burdens [1]. Despite the robust regenerative capacity of PNI induced by trauma, chronic diseases, surgical complications, and other etiologies, the regeneration process is notably slow. Furthermore, the local adverse environment can result in partial loss of sensory and motor functions as well as neuropathic pain [2, 3]. The degree of nerve regeneration is closely related to the formation and maturity of myelin sheaths [4]. As glial cells in the peripheral nervous system, Schwann cells(SCs) facilitate the regeneration of the myelin sheath around peripheral axons after PNI, thereby coordinating the response to nerve damage [5].

The proliferation and migration ability of SCs after PNI are regulated by local neural mechanical signals. In recent years, the role of mechanical signals in peripheral nerve diseases has emerged as a prominent area of research, particularly in the context of nerve development [6]. The local mechanical microenvironment undergoes significant alterations, prompting mechanosensitive cells to respond to mechanical stimuli and initiate a cascade of signal transduction events after PNI [7]. The mechanical properties changes of the physical environment of Schwann cells in the injured nerve area after PNI, such as increased hardness caused by local scar formation, and changes in substrate stiffness of SCs may activate the mechanical sensor Piezo1 [8]. As an ion channel directly gated by mechanical force, The extensive expression and activation of the Piezo1 channel in the neuromuscular skeletal system render it a promising therapeutic target for enhancing regeneration following injury [9]. Piezo1 is capable of detecting alterations in the biomechanical microenvironment of both neuronal and non-neuronal cells, subsequently mediating the passage of various cations particularly Ca^{2+} and a series of intracellular signaling pathways [10–12]. Research has demonstrated that Piezo1 functions as a negative regulator of myelination in SCs [13]. This may be related to the increased Piezo1 and Ca^{2+} influx after nerve injury, which may lead to the inactivation of downstream transduction signals TAZ/YAP [14, 15]. Yes-associated protein (YAP), transcriptional coactivator with PDZ-binding motif (TAZ) are key transcriptional co activators in the Hippo pathway, which nuclear level changes significantly affect the fate transition of cells from proliferation to differentiation, regeneration, and post injury repair [16, 17]. They could convey alterations in cytoskeletal tension to the nucleus [18]. During the differentiation and maturation of Schwann cells, YAP/TAZ was required to promote myelination [19, 20]. The process of cellular mechanotransduction, which involves the conversion of mechanical signals into biochemical signals, is a crucial regulatory mechanism in various biological processes [21]. Consequently, the development of mechanical therapies aimed at improving the local mechanical microenvironment represents a crucial aspect of PNI treatment.

Tuina is based on the basic theory of traditional Chinese medicine, and acupoints are selected according to syndrome differentiation, which has obvious therapeutic advantages in clinical chronic common diseases such as motor system, nervous system [22, 23]. Researches showed that "Three-Manipulation and Three-Acupoint" is the safe and effective Tuina method for PNI [24]. Previous basic researches had proved that Tuina could promote axonal regeneration and improve motor dysfunction and pain [25, 26]. Tuina is characterized by forceful acupoint stimulation that directly impacts subcutaneous tissue and nerve endings. Typically, this mechanical load induces alterations in the local mechanical microenvironment [27]. This study aimed to investigate whether Tuina could convert mechanical load into cellular responses via Piezo1, subsequently modulating the expression of mechanotransduction molecules YAP and TAZ to facilitate SCs proliferation and myelin regeneration.

By establishing a model of sciatic nerve injury (SNI), the research explored whether Tuina could change the expression of Piezo1/YAP/TAZ in the sciatic nerve to promote SCs proliferation and myelin regeneration which provides more evidence for Tuina to treat PNI.

Materials and methods

Animals and study design

A total of 24 specific-pathogen-free Sprague-Dawley male rats, weighing 200 ± 10 g, were obtained from Beijing Sibeifu Experimental Animal Research Institute Ltd (Beijing, China, Certificate Number: SCXK(JING) 2019-0010). All animals were kept in a room with a 12 h light/dark cycle, a constant temperature of 23 ± 2 °C, humidity of 45 ± 5%. The experimental procedures carried out on animals were approved and reviewed by the Experimental Animal Ethics Sub-Committee, Academic Committee of Beijing University of Chinese Medicine (Approval number: BUCM-2023121601-4205). All animal experiments were conducted according to the Guidelines of the NIH for the welfare of laboratory animals.

The animals were randomly divided into four groups: sham-operated (Sham) group, SNI group, Tuina group and Tuina + GsMTx4 group (6 rat/group).

Induction of SNI rats

The sciatic nerve crush injury rat model was established as previously described [28]. Briefly, rats were anesthetized with gas anesthesia machine. The right sciatic nerve was exposed using the gluteal-splitting approach after skin preparation. Sciatic nerves at the mid-thigh level

were exposed and crushed using a pair of non-serrated forceps for 5 s and the damage points about 2 mm. Subsequently, the skin was sutured with stitches. In Sham group, the nerve was only exposed without clamping.

Tuina interventions

The Tuina group and Tuina + GsMTx4 group received "Three-Manipulation and Three-Acupoint" intervention. The SNI group and the Sham group were subjected to restraint of the same duration. We used a Tuina manipulation emulator designed by our team to intervent (Patent number: ZL202320511277.5). The manipulator was designed to stimulate Tuina techniques, yet at the same time to also maintain qualitative and quantitative control. According to the "Three-Manipulation and Three-Acupoint": the emulator was used to perform the Dian, Bo, and Rou methods on Yinmen (BL37), Chengshan (BL57) and Yanglingquan (GB34) sequentially on the affected side, thereby using three different Tuina methods at three acupoints. A frequency of 60 times/minute and a force of 4 N were selected. Each Tuina method was applied for 1 min on each acupoint respectively and in total duration is 9 min. Tuina treatment was administered once daily for 20 days. In Tuina + GsMTx4 group, GsMTx4(50μmol/L) 60μL was stratified injected into the three acupoints 30 mins before Tuina intervention [29].

Gait analysis

Behavioral assessment was fulfilled by gait analysis based on the plantar imprinting using the Gait Analyzer (Zhongshi Science & Technology, Beijing, China). By analyzing the gait of rats with plantar imprinted walking, the SFI was used to assess the motor function recovery of the injured sciatic nerve. The lower SFI indicates more severe functional impairment of sciatic nerve. Three parameters, including toe spread (TS, first to the fifth toe), intermediate toe spread (ITS, second to the fourth toe), and total print length (PL, tip of the third toe to heel) were calculated to determine SFI as follows (E: experimental lateral; N: normal lateral):

$$SFI = -38.3((EPL\text{-}NPL)/NPL) + 109((ETS\text{-}NTS)/NTS) + 13.3((EITS\text{-}NITS)/NITS) - 8.8.$$

Mechanical withdrawal threshold(MWT)

The MWT of rats in each group was measured by BIO-EVF5 Von Frey pain measuring instrument. Rats were put into a transparent rat box with a baffle and a grid on the bottom, adapted for 15 ~ 30 min and detected after their exploration activities basically disappeared. Move the probe of the pain measuring instrument to the center of the right sole of the rat, continuously increase the pressure linearly, and record the threshold displayed by the instrument when the rat lifts and licks its foot. Each rat was measured 3 times with an interval of 5 min.

Electrophysiological test

The BL-420 S biological function system was used to directly measure the compound action potential (CMAP) of the right sciatic nerve in rats. Electrophysiological test was tested after intervention. The sciatic nerve was exposed after anesthesia with isoflurane. The recording electrode was inserted into the gastrocnemius muscle abdomen, and the grounding electrode was inserted into the rat's tail. The stimulating electrode was placed at the proximal end of the bridging nerve in turn, and the current was set at 1.0 mA. Click the instrument button to stimulate the nerve, record the amplitude and latency of CMAP.

Shear wave elastography (SWE) examination

SWE was used to dynamically observe the hardness changes of rat's sciatic nerve compression. The rats were taken to the lateral position, and the hind legs on the inspection side were upward, showing a natural relaxation state. Ultrasonic probe scans continuously from top to bottom along the anatomy of sciatic nerve. Apply a proper amount of coupling agent between probes during SWE to avoid the influence of sensor compression effect on the measured value. After obtaining a stable and satisfactory ultrasonic image of the superposition of elastic information, the nerve compression area is selected for measurement, and the shape of the nerve tissue in the area of interest is perpendicular to the direction of the sound beam as far as possible, and the measurement area is fixed at 0.01 cm [2], and the edge of the sampling frame is placed in the nerve adventitia, so as to measure the elastic velocity of the shear wave for three times respectively and record the average value.

Morphological examination

Toluidine blue staining was performed to observe the morphological changes of axon and myelin sheath in nerve fibers. The distal sciatic nerves of rats were taken and fixed overnight with 2.5% glutaraldehyde, fixed with 1% osmium tetroxide for 2 h at 4 °C, dehydrated in ethanol, and embedded in paraffin. The sections with a thickness of 4 μm were prepared, stained with 0.5% toluidine blue for 30 min, washed with water, immersed in 20% acetic acid, washed 3 times, sealed and observed. The structure and permutation distribution of axon and myelin sheath in nerve fibers were observed under an optical microscope (Olympus, Japan), and the number of myelinated nerve fibers was calculated using the Image J software.

Immunofluorescence staining (IF)

The expressions of YAP, TAZ and S100 calcium-binding protein β(S100β) in injured nerve tissue were detected by IF. After perfusion with 4% paraformaldehyde, the sciatic

nerve of the affected side was taken, embedded by OCT, cut into sections with a thickness of 6 μm, and sealed with goat serum at 37 for 30 min. Then incubated with rabbit anti-YAP antibody (1:500, Bioss, Beijing, China), rabbit anti-TAZ antibody (1:500, Bioss, Beijing, China), mouse anti- S100β antibody (1:1000, Bioss, Beijing, China) at 4 overnight. After rewarming, the sections were washed with PBS for three times, then added with secondary antibody (fluorescent labeled goat anti-mouse IgG 1:200, goat anti-rabbit IgG 1:200, Servicebio, Wuhan, China) for 2 h and washed with PBS for three times. The sections were then sealed with anti-fluorescence quenching sealing tablets and observed under a Fluorescence microscope (Olympus, Japan). Images were captured, and the fluorescence intensity of the target protein was measured using the Image J software.

Western blot (WB) analysis

The protein expression of Piezo1, Myelin basic protein (MBP) and Neurofilament 200 (NF200) in damaged nerves was detected by WB. After grinding the nerves, RIPA lysate was added and centrifuged for 20 min at the following conditions: 12,000 rpm/min at 4 ° C. The supernatant was taken and protein concentration was determined by the BCA method; the protein is denatured at 95 °C. Following denaturation, proteins were separated using polyacrylamide gel electrophoresis. Proteins were transferred from the gel onto the PVDF membranes and blocked with 5% nonfat dry milk for 2 h. The PVDF membranes were incubated with the first antibody β-actin (1:2000, Servicebio, Wuhan, China), Piezo1 Antibody (1:1000, Affinity Biosciences, OH, USA), NF200 Antibody (1:2000, Bioss, Beijing, China) and MBP Antibody (1:1000, Bioss, Beijing, China) for overnight at 4 °C. The secondary antibody (HRP labeled goat anti-mouse 1:10,000, HRP-labeled goat anti-rabbit 1:10,000, Servicebio, Wuhan, China) were incubated at room temperature for 1 h. The membranes were exposed to Electrochemiluminescence (ECL) in a darkroom. Image J software was used to analyze the gray level of the target strip of the scanned image, and the results were calculated by β-actin.

Real-Time quantitative PCR(RT-PCR)

The mRNA expressions of Piezo1, YAP and TAZ in injured nerves were detected by RT-PCR. Take a proper amount of nerve tissue in the ultra-clean platform environment, extract the tissue RNA with the tissue cell RNA extraction box, and then reverse transcribe the RNA into cDNA with the cDNA first-strand synthesis kit for amplification. Primer sequence number: GAPDH upstream primer: CTGGAGAAACCTGCCAAGTATG, downstream primer: GGTGGAAGAATGGGAGTTGCT; Piezo1 upstream primer: AGCAAGCAGGCACAAAGGC, downstream primer: CGCACAAACTTGCCAACGAC; YAP upstream primer: GACAACAACATGGCAGGACCC, downstream primer: TGAGGCAGAGTTCATCAGCGT; TAZ upstream primer: TCCTGCGACCCCTCTTATCA, downstream primer: CAGCTCCTTGGTGAAGCAGA. After amplification, the relative expression was calculated according to $2^{-\triangle\triangle Ct}$ method.

Calcium assay kit

Accurately weigh the nerve tissue, add deionized water according to the ratio of weight (g): volume (mL) = 1:9, homogenize in ice water bath, centrifuge at 2500 rpm for 10 min, and take 10% homogenate supernatant to be tested. The samples were detected according to kit procedures (Nanjing Jiancheng Bioengineering Institute, Nanjing, China), and the absorbance values were measured at 610 nm. The contents of Ca^{2+} were calculated by comparing them with the standard substance. Three wells were set for each index.

Statistical analysis

All data were analyzed by SPSS 20.0 statistical software, and the experimental data were described as mean ± Standard deviation (SD). One-Way ANOVA followed by LSD was used for comparisons between groups that were normally distributed and had equal variance. Tamhane's T2 method was used for comparisons between multiple groups that were normally distributed and did not have homogeneous variance. A value of $P < 0.05$ was considered statistically significant. Higher significance levels were established at $P < 0.01$.

Results

Tuina facilitated the recovery of neurological function in SNI rats

In order to evaliate the impact of Tuina on the neurological function of SNI rats, assessments such as SFI, MWT and sciatic nerve electrophysiology of rats were conducted. The results showed that the SFI of SNI group was significantly lower than that of Sham group ($P < 0.01$). SFI of Tuina group was significantly higher than that of SNI group ($P < 0.01$), and SFI of Tuina + GsMTx4 group was significantly lower than Tuina group ($P < 0.01$). (Fig. 1A and B) MWT of SNI group was significantly lower than that of Sham group ($P < 0.01$), MWT of Tuina group was significantly higher than that of SNI group ($P < 0.01$), and MWT of Tuina + GsMTx4 group was significantly lower than Tuina group ($P < 0.01$). (Fig. 1C) Compared with Sham group, CMAP latency was significantly increased and CMAP amplitude was significantly decreased in SNI group ($P < 0.01$); compared with SNI group, CMAP latency was significantly decreased and CMAP amplitude was significantly increased in Tuina group ($P < 0.01$); Compared with Tuina group, the CMAP latency of

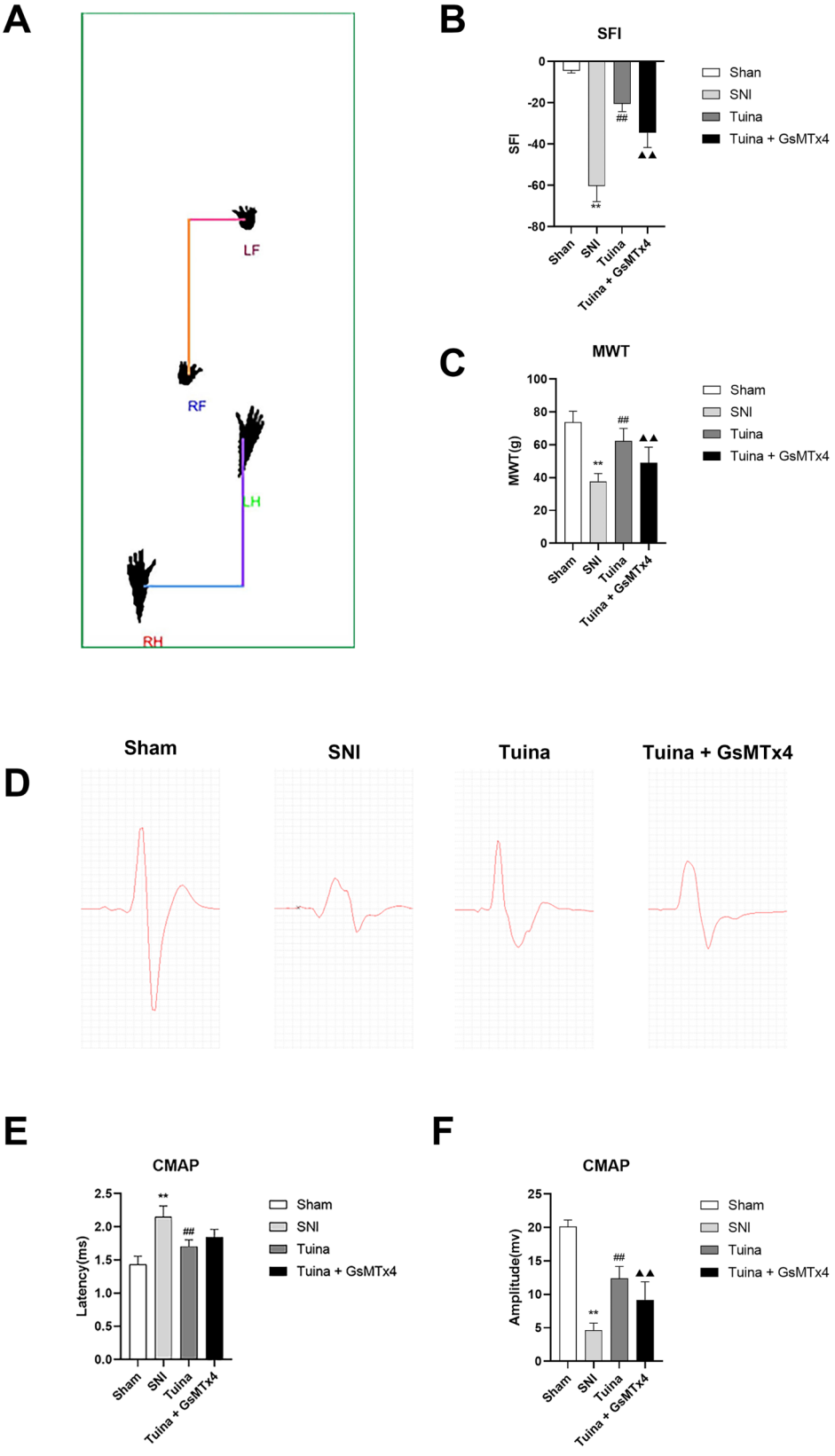

Fig. 1 Tuina facilitated the recovery of neurological function in SNI rats. **(A)** Representative images of footprints of rats. **(B)**The mean SFI in each group. ($n=6$) ** $P<0.01$ vs. the Sham group. $^{\#\#}P<0.01$ vs. the SNI group. $^{\blacktriangle\blacktriangle}P<0.01$ vs. the Tuina group. **(C)**The mean MWT in each group. ($n=6$) ** $P<0.01$ vs. the Sham group. $^{\#\#}P<0.01$ vs. the SNI group. $^{\blacktriangle\blacktriangle}P<0.01$ vs. the Tuina group. **(D)** Representative images of electrophysiological test in each group. **(E)**& **(F)** CMAP changes between groups. ($n=6$) ** $P<0.01$ vs. the Sham group. $^{\#\#}P<0.01$ vs. the SNI group. $^{\blacktriangle\blacktriangle}P<0.01$ vs. the Tuina group.

Tuina + GsMTx4 group was increased and the CMAP amplitude was significantly decreased ($P > 0.05$, $P < 0.01$). (Fig. 1D, E and F)

Tuina improved the mechanical environment of injured nerves in SNI rats

To investigate this effect, SWE was employed to examine the right sciatic nerve (Fig. 2A), and the expression levels of Piezo1, Ca^{2+}, YAP and TAZ were measured. The results of SWE showed that Emax and Smax of sciatic nerve in SNI group were significantly higher than Sham group ($P < 0.01$). Compared with SNI group, the Emax and Smax of sciatic nerve in the Tuina group were significantly decreased ($P < 0.01$). Compared with Tuina group, the Emax and Smax of sciatic nerve in Tuina + GsMTx4 group increased, but there was no statistical difference ($P > 0.05$). (Fig. 2B and C) The results of WB, RT-PCR and Calcium Assay Kit showed that the expression of Piezo1 protein, Piezo1 mRNA and Ca^{2+} in sciatic nerve in SNI group were significantly higher than those in Sham group ($P < 0.01$). The expression of Piezo1 protein, Piezo1 mRNA and Ca^{2+} in the sciatic nerve of the Tuina group were significantly lower than those of SNI group ($P < 0.01$). The expression of Piezo1 protein and Piezo1 mRNA in Tuina + GsMTx4 group were higher than Tuina group ($P < 0.05$, $P < 0.01$), and the concentration of Ca^{2+} was higher than Tuina group, but there was no statistical difference ($P > 0.05$). (Fig. 2D, E, F and G) The results of RT-PCR and IF showed that the Average Optical Density(AOD) and mRNA expression of YAP and TAZ in SNI group were significantly lower than Sham group ($P < 0.01$). (Fig. 3A and D) Compared with SNI group, the AOD and mRNA expression of YAP and TAZ in the Tuina group increased significantly ($P < 0.01$). Compared with the Tuina group, the mRNA expression of YAP, the AOD and mRNA expression of TAZ in Tuina + GsMTx4 group decreased significantly ($P < 0.01$, $P < 0.05$), (Fig. 3C, E and F) and the AOD of YAP showed a decreasing trend, but there was no statistical difference ($P > 0.05$) (Fig. 3B).

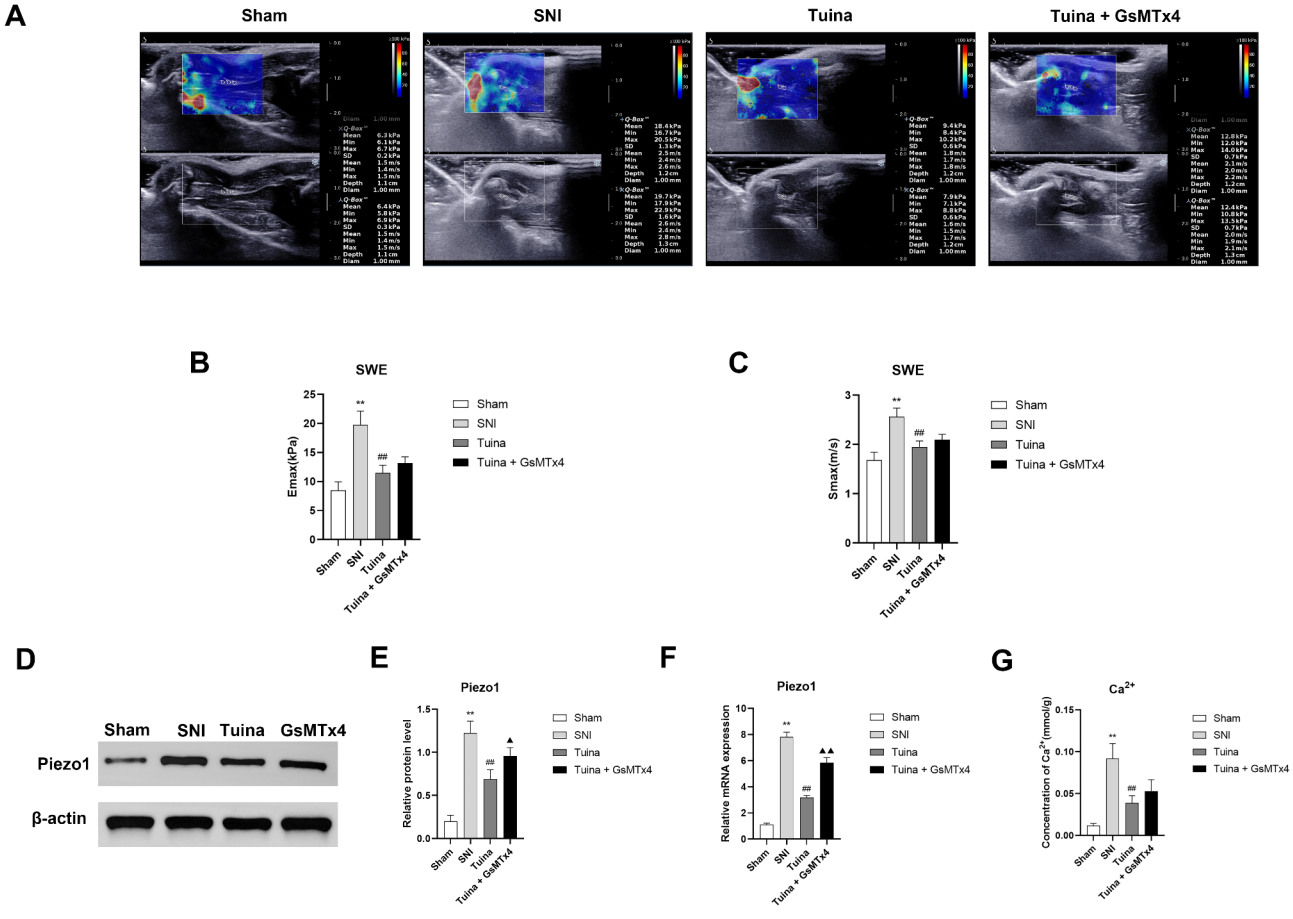

Fig. 2 Tuina improved the mechanical environment of injured nerves in SNI rats. **(A)** Representative SWE images in each group. **(B)**& **(C)** Emax and Smax changes between groups. ($n = 3$) ** $P < 0.01$ vs. the Sham group. $^{\#\#}P < 0.01$ vs. the SNI group. **(D)** Typical protein bands of Piezo1. **(E)** Protein level comparison of Piezo1 between groups. ($n = 3$) ** $P < 0.01$ vs. the Sham group. $^{\#\#}P < 0.01$ vs. the SNI group. $^{\blacktriangle}P < 0.05$ vs. the Tuina group. Data were analyzed by Image J. **(F)** Relative mRNA expression of Piezo1 between groups. ($n = 3$) ** $P < 0.01$ vs. the Sham group. $^{\#\#}P < 0.01$ vs. the SNI group. $^{\blacktriangle\blacktriangle}P < 0.01$ vs. the Tuina group. **(G)** Concentration of Ca^{2+} between groups. ($n = 6$) ** $P < 0.01$ vs. the Sham group. $^{\#\#}P < 0.01$ vs. the SNI group.

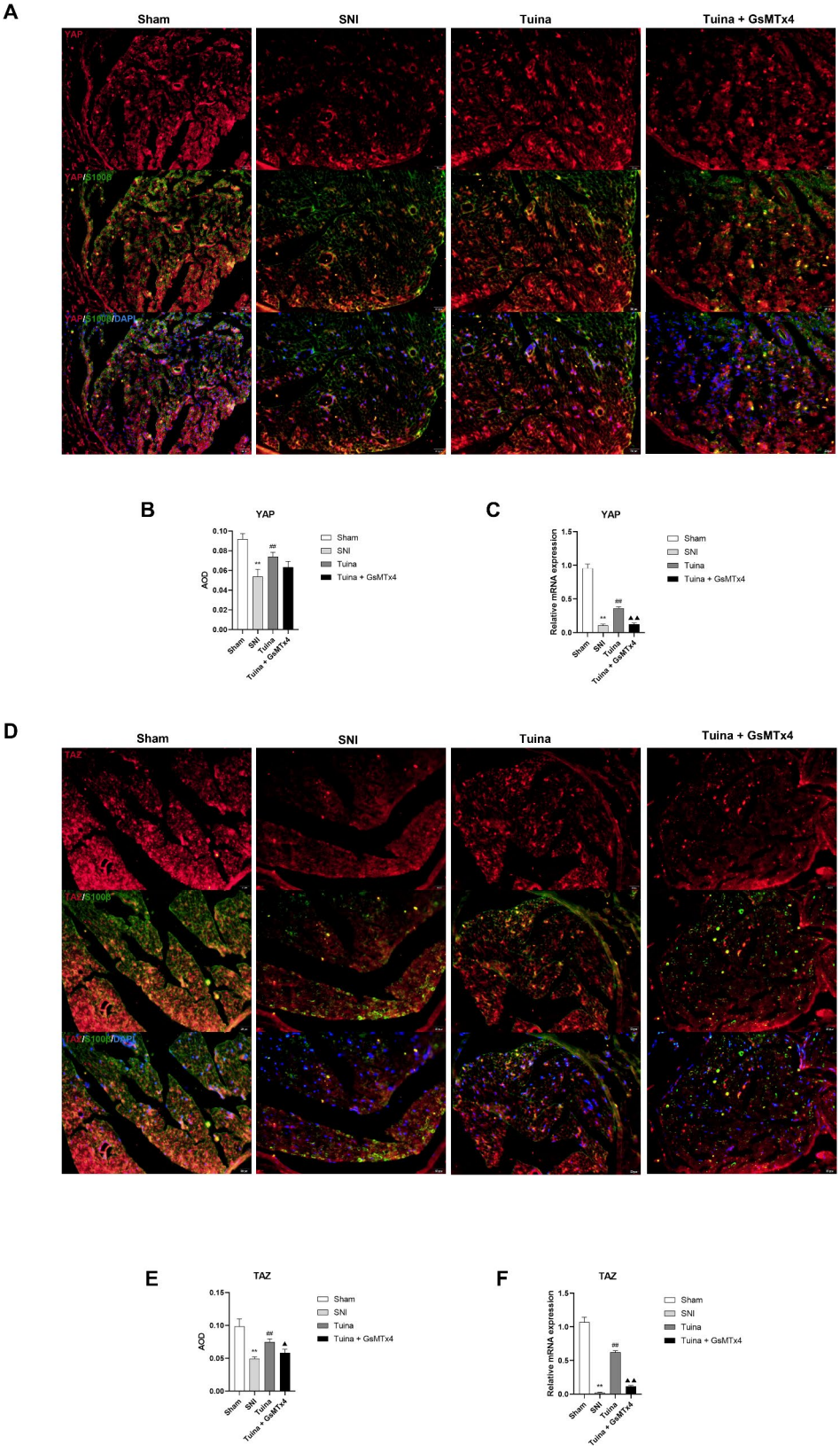

Fig. 3 (See legend on next page.)

(See figure on previous page.)

Fig. 3 Tuina improved the mechanical environment of injured nerves in SNI rats. **(A)** Representative YAP and S100β IF sections of nerve tissues in each group, 400×. **(B)** Average Optical Density (AOD) value of YAP in each group. ($n=3$) Data were analyzed by Image J. ** $P<0.01$ vs. the Sham group. $^{\#\#}P<0.01$ vs. the SNI group. **(C)** Relative mRNA expression of YAP between groups. ($n=3$) ** $P<0.01$ vs. the Sham group. $^{\#\#}P<0.01$ vs. the SNI group. $^{\blacktriangle\blacktriangle}P<0.01$ vs. the Tuina group. **(D)** Representative TAZ and S100β IF sections of nerve tissues in each group, 400×. **(E)** AOD value of TAZ in each group. ($n=3$) Data were analyzed by Image J. ** $P<0.01$ vs. the Sham group. $^{\#\#}P<0.01$ vs. the SNI group. $^{\blacktriangle}P<0.05$ vs. the Tuina group. **(F)** Relative mRNA expression of TAZ between groups. ($n=3$) ** $P<0.01$ vs. the Sham group. $^{\#\#}P<0.01$ vs. the SNI group. $^{\blacktriangle\blacktriangle}P<0.01$ vs. the Tuina group.

Tuina promoted axonal regeneration of injured nerve in SNI rats

In order to observe the effect of Tuina on axonal regeneration of injured nerve in SNI rats, we stained sciatic nerve with toluidine blue, and detected MBP, NF200 and S100β in nerve. Toluidine blue staining showed that well-arranged myelinated fibers were apparent without inflammatory cells or vacuolation in Sham group; In SNI group, the sciatic nerve fibers and myelin sheathes were disarranged, the vacuolation areas was observed more than Sham groups, and the number of myelinated nerve fibers decreased ($P<0.01$). The number of myelinated nerve fibers in Tuina group was increased compared with SNI group ($P<0.01$). Compared with Tuina group, the number of myelinated nerve fibers in Tuina + GsMTx4 group decreased ($P<0.01$). (Fig. 4A and B) The results of WB and IF showed that compared with Sham group, the protein expression of MBP and NF200 in sciatic nerve in SNI group was significantly decreased ($P<0.01$) (Fig. 4C), and the AOD of S100β was also significantly decreased ($P<0.01$) (Fig. 4G). Compared with SNI group, the protein expression of MBP and NF200 in the sciatic nerve in Tuina group increased significantly ($P<0.01$) (Fig. 4D and E), and the AOD of S100β also increased ($P<0.01$) (Fig. 4F). Compared with Tuina group, the protein expression of MBP in sciatic nerve of Tuina + GsMTx4 group was decreased ($P<0.05$), the protein expression of NF200 was decreased but there was no statistical difference ($P>0.05$), and the AOD of S100β was decreased ($P<0.01$).

Discussion

This study demonstrated that the substrate hardness of locally damaged nerves changes after SNI. Specifically, there is an abnormal increase in the mechanically sensitive ion channel Piezo1, an elevated Ca^{2+} influx, inactivation of the YAP/TAZ pathway, the process of SCs proliferation and myelination is blocked. Tuina intervention had been shown to facilitate SCs proliferation, myelin regeneration and nerve repair through the Piezo1/YAP/TAZ pathway.

SNI model is one of the most commonly used models of PNI due to the surgical approach of sciatic nerve is convenient and easy to separate [30]. The mechanical compression model of sciatic nerve could interrupt axons and fasciculus without interrupting nerve continuity, causing Sunderland III-IV nerve injury [31, 32]. We continued to utilize this model since it is reliable and widely used. Tuina is an effective method to treat PNI in clinic, and "Three-Manipulation and Three-Acupoint" was effective prescriptions to treat PNI [33]. The three acupoints conform to the principle of selecting points along the meridian and selecting points locally in traditional Chinese medicine, and at the same time form a "point-nerve-muscle" related area with local nerves and muscles, which could stimulate nerves and muscles at the same time [34, 35]. The three methods correspond to the working habits of clinical practical application. As a result, this study continued to choose "Three-Manipulation and Three-Acupoint" intervention to investigate the mechanism of Tuina treatment of PNI.

Electrophysiological tests, MWT and SFI assessments indicated that Tuina exerts a therapeutic effect on SNI. Both SFI and MWT are crucial indices for evaluating functional recovery post-SNI [36, 37]. The findings indicated that Tuina intervention could significantly ameliorate motor dysfunction following SNI and alleviate associated neuropathic pain. CMAP serves as a critical metric for assessing the efficacy of electrical conduction between peripheral nerves and their corresponding motor units, with its amplitude and latency being closely correlated with the effective electrical transmission between nerves and skeletal muscles [38]. The results demonstrated a progressive recovery in the effective electrical conduction between the sciatic nerve and skeletal muscle post-Tuina intervention. The aforementioned results demonstrated that Tuina intervention facilitates the recovery of injured nerves and ameliorates motor and sensory dysfunction in affected offspring.

Tuina intervention promoted the regrowth of the myelin sheath in injured nerves and accelerates axonal regeneration. Following PNI, Wallerian degeneration occurs at the distal end of the nerve [39]. In response, SCs are activated to secrete growth factors, thereby providing channels for nerve regeneration. S100β is a protein expressed by SCs that plays a crucial role in this regenerative process [40, 41]. The IF results demonstrated an upregulation of S100β expression following Tuina intervention, suggesting that Tuina promoted the activation and differentiation of SCs. MBP, a critical component of the myelin sheath, serves as an indicator of myelin sheath integrity, with its dynamics reflecting the extent of nerve damage [42]. NF200, a cytoskeletal protein in nerve cells, provides comprehensive visualization of the morphology

and distribution of entire nerve cells [43]. The findings of this study indicated a reduction in MBP and NF200 levels in SNI group, implying that SNI led to myelin sheath degradation and axonal damage. However, the levels of MBP and NF200 in Tuina group were significantly elevated compared to SNI group, suggesting that Tuina facilitates the proliferation and differentiation of SCs and the regeneration of the myelin sheath, thereby promoting axonal growth in injured nerves. This was further corroborated by Toluidine blue staining, which demonstrated changes in the myelin sheath and axon. The regeneration of injured nerves is contingent upon the capacity for axonal regeneration [44]. These findings indicated that Tuina enhances axonal regeneration in injured nerves through myelin sheath repair, thereby improving functional outcomes.

Tuina intervention promoting myelin sheath repair may be related to Tuina improving the local mechanical environment of damaged nerves and acting on the electrochemical signal transduction pathway Piezo1/YAP/TAZ. Tuina intervention facilitated axonal regeneration in injured nerves by altering the local mechanical microenvironment at the site of nerve injury. SWE could measure tissue stiffness through the propagation of shear waves, thereby objectively reflecting the pathological characteristics of the tissue and quantifying the biomechanical properties of the sciatic nerve [45]. The results indicated that the shear wave velocity of the sciatic nerve increases in the SNI group, suggesting a change in the local mechanical environment of the sciatic nerve and increased neural hardness. Tuina intervention reversed this trend, demonstrating an improvement in the local mechanical environment of the sciatic nerve. The Piezo channel transduces mechanical stimuli into electrical and chemical signals, thereby influencing development, tissue homeostasis, and regeneration, and playing a critical role in physiological sensory conduction in mammals [46]. Research had demonstrated that Piezo1 is instrumental in inhibiting axon regeneration in nervous system pathologies, affecting processes such as neuronal repair, SCs proliferation, and neural stem cell differentiation [47–49]. Notably, both Piezo1 and Ca^{2+} levels were significantly elevated in the SNI group, corroborating findings from previous studies [8]. After nerve injury, local fibrosis leads to increased hardness. The interaction between the local growth cone and glial cells following nerve injury generates mechanical force, potentially leading to the activation of the Piezo1 channel in SCs [50, 51]. Piezo1 activation resulted in a localized increase in calcium ions and a sequence of cascade reactions that restrict axonal regrowth. As a mechanical stimulus, the Tuina intervention targeted acupoints situated along the nerve trunk, thereby altering the mechanical microenvironment of the entire nerve. Concurrently, this mechanical stimulus could be detected by local mechanosensitive ion channels, which transduce mechanical signals into electrical signals, thereby modulating the local signals at the site of injury [52]. The differential expression of Piezo1 in Tuina + GsMTx4 group compared to Tuina group further substantiates this point. GsMTx4, a gating modifier peptide derived from spider venom, is known for its selective inhibition of cation-permeable mechanosensitive channels (MSCs) within the Piezo and TRP channel families [53]. In Tuina + GsMTx4 group, mechanical signals were unable to be transduced into electrical signals following the injection of inhibitors into acupoints. Consequently, the biomechanical transduction mechanisms underlying Tuina failed to initiate the anticipated neuromodulatory cascade required for therapeutic efficacy. The inability to convert mechanical signals may account for the poor functional recovery and lack of significant nerve axon regeneration observed in Tuina + GsMTx4 group.

Piezo1 is involved in nerve regeneration via Ca^{2+} signaling, which subsequently induces the phosphorylation, localization, and regulation of the nuclear activity of YAP/TAZ. YAP/TAZ functions as a mechanotransducer, capable of transmitting mechanical signals to the nucleus to initiate a series of cellular responses [54]. In SCs, YAP/TAZ was responsive to extracellular mechanical cues, a sensitivity that is crucial for the dedifferentiation, proliferation, and regeneration of the myelin sheath following PNI [55, 56]. Grove et al. have demonstrated that YAP/TAZ facilitates the differentiation of immature SCs and that YAP/TAZ expression markedly diminishes in SCs of adult mice following axonal injury, only reappearing if axonal regeneration occurs [57, 58]. The Piezo1 channel influences the activation and regulation of YAP/TAZ in SCs, with both YAP and TAZ recently identified as downstream effector molecules of Piezo1 channel activity [13, 59]. In this study, the expression levels of YAP and TAZ in the nerve tissue of SNI group were significantly reduced, whereas those in Tuina group were significantly elevated. This phenomenon may be attributed to Tuina as a mechanical stimulation, which could reduce the abnormal increase in hardness of damaged nerves, decrease the abnormal activation of Piezo1 and facilitate the influx of calcium ions. This cascade activated YAP/TAZ, which is closely related to myelin formation, prompted its translocation to the nucleus and inducing the proliferation of SCs along with a series of cellular activities. Based on the results of the Tuina + GsMTx4 group, we speculated that Tuina as a mechanical stimulus, was related to the transduction of local mechanical signals. After local injection of inhibitors at acupoints, the mechanical stimulation of Tuina could not be perceived and transmitted, and could not participate in the regulation of the local neural mechanical environment. This may be the reason why the Tuina + GsMTx4 group had significant differences in

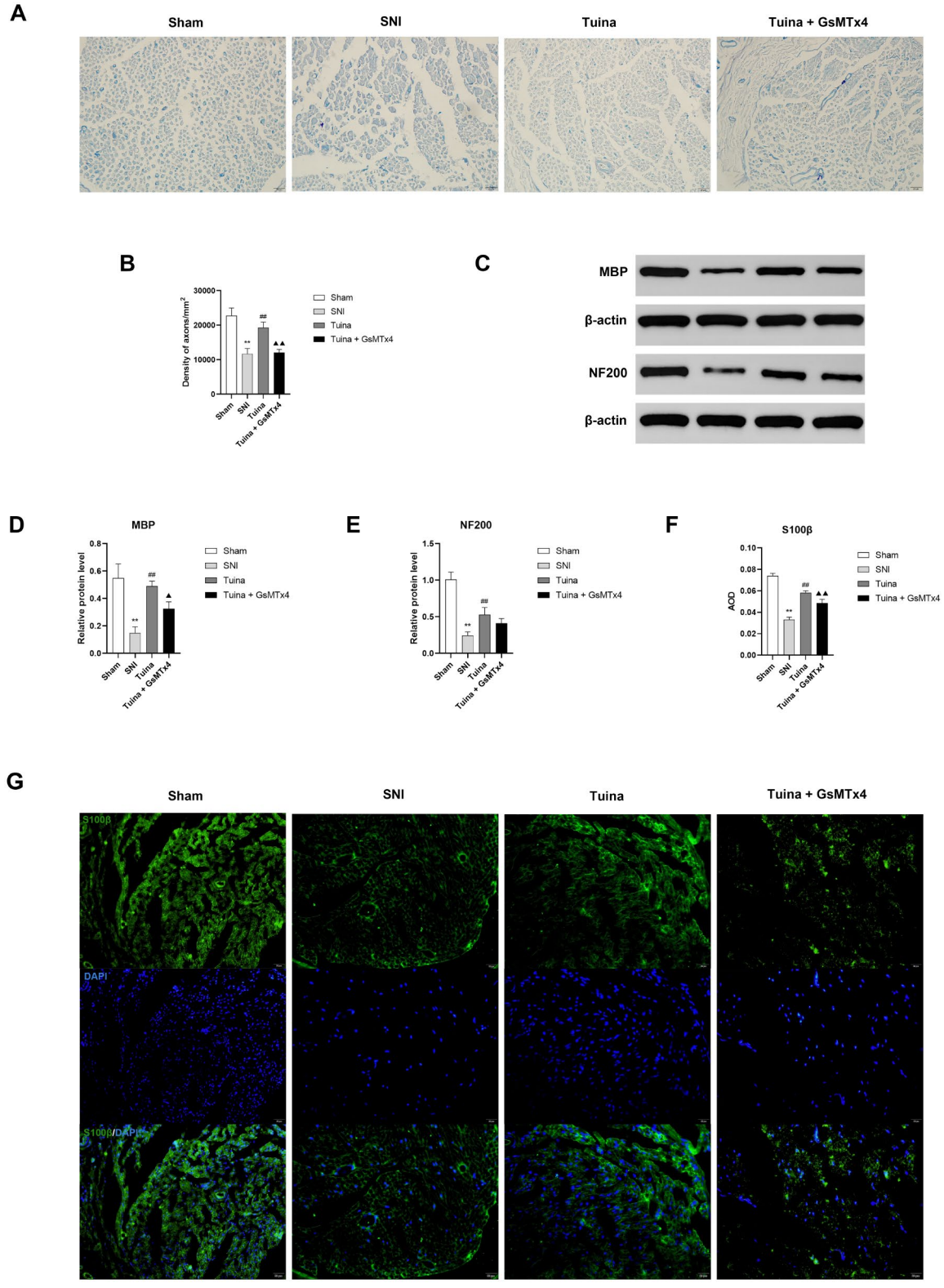

Fig. 4 Tuina promoted axonal regeneration of injured nerve in SNI rats. **(A)** Representative nerve tissues of each group stained with Toluidine blue staining, 400×. **(B)** Density of axons of each group. ($n=3$) ** $P<0.01$ vs. the Sham group. $^{\#\#}P<0.01$ vs. the SNI group. $^{▲▲}P<0.01$ vs. the Tuina group. **(C)** Typical protein bands of MBP and NF200. **(D)**& **(E)** Protein level comparison of MBP and NF200 between groups. ($n=3$) ** $P<0.01$ vs. the Sham group. $^{\#\#}P<0.01$ vs. the SNI group. $^{▲}P<0.05$ vs. the Tuina group. Data were analyzed by Image J. **(F)** AOD value of S100β in each group. ($n=3$) Data were analyzed by Image J. ** $P<0.01$ vs. the Sham group. $^{\#\#}P<0.01$ vs. the SNI group. $^{▲▲}P<0.01$ vs. the Tuina group. **(G)** Representative S100β IF sections of nerve tissues in each group, 400×

function, myelin regeneration degree, and mechanical transduction signals compared to the Tuina group.

This study has some limitations. We have not studied the changes in the local neuromechanical environment after injury at the cellular level. Therefore, the changes of mechanical microenvironment would be further explained from different levels in the future.

Conclusion

This study demonstrated that the regeneration of damaged nerve myelin sheaths post-Tuina intervention are associated with alterations in the Piezo1/YAP/TAZ signaling pathway within SCs, induced by the mechanical forces generated through Tuina.

Abbreviations

PNI	Peripheral nerve injury
SCs	Schwann cells
IF	Immunofluorescence
WB	Western Blot
RT-PCR	Real-Time Quantitative PCR
SFI	Somatic Functional Index
MWT	Mechanical Withdrawal Threshold
SWE	Shear wave elastography
CMAP	Compound action potential

Author contributions

Yue Xu and Na Rentuya designed of the work and wrote the main manuscript text, Tianyuan Yu and Yingqi Zhang have drafted the work, Jiawang Yan and Hongzheng Zhang prepared figures1-4, Hanyu Zhang and Jiawei Sun and Jiayue Liu have made substantial contributions to the interpretation of data. All authors reviewed the manuscript.

Funding

This work was supported by the China National Natural Science Foundation (82274675) and Beijing National Natural Science Foundation (7232278).

Data availability

No datasets were generated or analysed during the current study.

Declarations

Competing interests

The authors declare no competing interests.

Disclosure

The authors report no conflicts of interest in this work.

Received: 16 December 2024 / Accepted: 7 April 2025
Published online: 12 May 2025

References

1. Lopes B, Sousa P, Alvites R, et al. Peripheral nerve injury treatments and advances: one health perspective. Int J Mol Sci Jan. 2022;14(2). https://doi.org/10.3390/ijms23020918.
2. Zhao Y, Liu Y, Kang S, et al. Peripheral nerve injury repair by electrical stimulation combined with graphene-based scaffolds. Front Bioeng Biotechnol. 2024;12:1345163. https://doi.org/10.3389/fbioe.2024.1345163.
3. Huang L, Bian M, Zhang J, et al. Iron metabolism and ferroptosis in peripheral nerve injury. Oxid Med Cell Longev. 2022;2022:5918218. https://doi.org/10.1155/2022/5918218.
4. Su Y, Huang M, Thomas AG et al. GCPII Inhibition Promotes Remyelination after Peripheral Nerve Injury in Aged Mice. Int J Mol Sci. 2024;25(13):6893. Published 2024 Jun 23. https://doi.org/10.3390/ijms25136893
5. Zhang Y, Zhao Q, Chen Q, et al. Transcriptional control of peripheral nerve regeneration. Mol Neurobiol Jan. 2023;60(1):329–41. https://doi.org/10.1007/s12035-022-03090-0.
6. Miles L, Powell J, Kozak C, et al. Mechanosensitive ion channels, axonal growth, and regeneration. Neuroscientist Aug. 2023;29(4):421–44. https://doi.org/10.1177/10738584221088575.
7. Kong L, Gao X, Qian Y, et al. Biomechanical microenvironment in peripheral nerve regeneration: from pathophysiological Understanding to tissue engineering development. Theranostics. 2022;12(11):4993–5014. https://doi.org/10.7150/thno.74571.
8. Liang J, Zhang N, Li G, et al. Piezo1 promotes peripheral nerve fibrotic Scar formation through Schwann cell senescence. Neurosci Lett Aug. 2024;10:837:137916. https://doi.org/10.1016/j.neulet.2024.137916.
9. Savadipour A, Palmer D, Ely EV, et al. The role of PIEZO ion channels in the musculoskeletal system. Am J Physiol Cell Physiol Mar. 2023;1(3):C728–40. https://doi.org/10.1152/ajpcell.00544.2022.
10. Pan Y, Shi LZ, Yoon CW, et al. Mechanosensor Piezo1 mediates bimodal patterns of intracellular calcium and FAK signaling. EMBO J Sep. 2022;1(17):e111799. https://doi.org/10.15252/embj.2022111799.
11. Coste B, Mathur J, Schmidt M, et al. Piezo1 and Piezo2 are essential components of distinct mechanically activated cation channels. Sci Oct. 2010;1(6000):55–60. https://doi.org/10.1126/science.1193270.
12. Chen X, Wanggou S, Bodalia A, et al. A feedforward mechanism mediated by mechanosensitive ion channel PIEZO1 and tissue mechanics promotes glioma aggression. Neuron Nov. 2018;21(4):799–e8157. https://doi.org/10.1016/j.neuron.2018.09.046.
13. Acheta J, Bhatia U, Haley J, et al. Piezo channels contribute to the regulation of myelination in Schwann cells. Glia Dec. 2022;70(12):2276–89. https://doi.org/10.1002/glia.24251.
14. Li F, Lo TY, Miles L, et al. The Atr-Chek1 pathway inhibits axon regeneration in response to Piezo-dependent mechanosensation. Nat Commun Jun. 2021;22(1):3845. https://doi.org/10.1038/s41467-021-24131-7.
15. Izhiman Y, Esfandiari L. Emerging role of extracellular vesicles and exogenous stimuli in molecular mechanisms of peripheral nerve regeneration. Front Cell Neurosci. 2024;18:1368630. https://doi.org/10.3389/fncel.2024.1368630.
16. Mo JS, Park HW, Guan KL. The Hippo signaling pathway in stem cell biology and cancer. EMBO Rep. 2014;15(6):642–56. https://doi.org/10.15252/embr.201438638.
17. Jeanette H, Marziali LN, Bhatia U, et al. YAP and TAZ regulate Schwann cell proliferation and differentiation during peripheral nerve regeneration. Glia Apr. 2021;69(4):1061–74. https://doi.org/10.1002/glia.23949.
18. Astone M, Tesoriero C, Schiavone M, et al. Wnt/β-Catenin signaling regulates Yap/Taz activity during embryonic development in zebrafish. Int J Mol Sci. 2024;25(18):10005. https://doi.org/10.3390/ijms251810005. Published 2024 Sep 17.
19. Wang J, Chen H, Hou W, et al. Hippo pathway in Schwann cells and regeneration of peripheral nervous system. Dev Neurosci. 2023;45(5):276–89. https://doi.org/10.1159/000530621.
20. Belin S, Zuloaga KL, Poitelon Y. Influence of mechanical stimuli on Schwann cell biology. Front Cell Neurosci. 2017;11:347. https://doi.org/10.3389/fncel.2017.00347.
21. Di X, Gao X, Peng L, et al. Cellular mechanotransduction in health and diseases: from molecular mechanism to therapeutic targets. Signal Transduct Target Ther Jul. 2023;31(1):282. https://doi.org/10.1038/s41392-023-01501-9.
22. Song P, Sun W, Zhang H, et al. Possible mechanism underlying analgesic effect of tuina in rats May involve piezo mechanosensitive channels within dorsal root ganglia axon. J Tradit Chin Med Dec. 2018;38(6):834–41.
23. Gong Z, Guo Y, Liu X, et al. Bibliometric analysis of research trends on tuina manipulation for neck pain treatment over the past 10 years. J Pain Res. 2023;16:2063–77. https://doi.org/10.2147/JPR.S410603.
24. Liu ZF, Wang HR, Yu TY, et al. Tuina for peripherally-induced neuropathic pain: A review of analgesic mechanism. Front Neurosci. 2022;16:1096734. https://doi.org/10.3389/fnins.2022.1096734.
25. Sachula, Yang Z, Yu T, et al. Exploring the mechanism of immediate analgesia induced by tuina intervention on minor chronic constriction injury in rats using LC-MS. J Pain Res. 2024;17:321–34. https://doi.org/10.2147/JPR.S438682.
26. Lyu T, Liu Z, Yu T et al. Applying RNA sequencing technology to explore repair mechanism of Tuina on gastrocnemius muscle in sciatic nerve injury rats. Chin Med J (Engl). Oct 5. 2022;135(19):2378–2379. https://doi.org/10.1097/CM9.0000000000001960

27. Chen J, Zhou R, Feng Y, et al. Molecular mechanisms of exercise contributing to tissue regeneration. Signal Transduct Target Ther Nov. 2022;30(1):383. https://doi.org/10.1038/s41392-022-01233-2.
28. Lv TT, Mo YJ, Yu TY, et al. Using RNA-Seq to explore the repair mechanism of the three methods and three-Acupoint technique on DRGs in sciatic nerve injured rats. Pain Res Manag. 2020;2020:7531409. https://doi.org/10.1155/2020/7531409.
29. Yu-jia LI,ZHENG, Ya-wen ZUO, Wei-min et al. Involvement of mechanosensitive Piezo channels at acupoints in the initiation mechanism of acupuncture analgesia on rat ankle arthritis. China Journal of Traditional Chinese Medicine and Pharmacy. 2023, 38 (06): 2908–2914.
30. Umansky D, Hagen KM, Chu TH, et al. Functional gait assessment using manual, Semi-Automated and deep learning approaches following standardized models of peripheral nerve injury in mice. Biomolecules Sep. 2022;23(10). https://doi.org/10.3390/biom12101355.
31. Ganguly A, McEwen C, Troy EL, et al. Recovery of sensorimotor function following sciatic nerve injury across multiple rat strains. J Neurosci Methods Jan. 2017;1:275:25–32. https://doi.org/10.1016/j.jneumeth.2016.10.018.
32. Yeoh S, Warner WS, Eli I, et al. Rapid-stretch injury to peripheral nerves: comparison of injury models. J Neurosurg Sep. 2021;1(3):893–903. https://doi.org/10.3171/2020.5.JNS193448.
33. Liu Z, Wang H, Yu T, et al. A review on the mechanism of tuina promoting the recovery of peripheral nerve injury. Evid Based Complement Alternat Med. 2021;2021:6652099. https://doi.org/10.1155/2021/6652099.
34. Wang H, Liu Z, Yu T, et al. Exploring the mechanism of immediate analgesic effect of 1-time tuina intervention in minor chronic constriction injury rats using RNA-seq. Front Neurosci. 2022;16:1007432. https://doi.org/10.3389/fnins.2022.1007432.
35. Yang Z, Sa C, Yu T, et al. Exploring the analgesic initiation mechanism of tuina in the dorsal root ganglion of minor CCI rats via the TRPV1/TRPA1-cGMP pathway. Pain Res Manag. 2024;2024:2437396. https://doi.org/10.1155/2024/2437396.
36. DeLeonibus A, Rezaei M, Fahradyan V, et al. A meta-analysis of functional outcomes in rat sciatic nerve injury models. Microsurgery Mar. 2021;41(3):286–95. https://doi.org/10.1002/micr.30713.
37. Liu C, Guo QL, Huang CS, et al. Suppressing SNAP-25 and reversing glial glutamate transporters relieves neuropathic pain in rats by ameliorating imbalanced neurotransmission. Chin Med J (Engl) Nov. 2013;126(21):4100–4.
38. Liu Y, Xu YJ. LKB1 and CRMP1 cooperatively promote the repair of the sciatic nerve injury. Dev Neurobiol Jan. 2024;84(1):18–31. https://doi.org/10.1002/dneu.22932.
39. Burnett MG, Zager EL. Pathophysiology of peripheral nerve injury: a brief review. Neurosurg Focus May. 2004;15(5):E1. https://doi.org/10.3171/foc.2004.16.5.2.
40. Ling J, He C, Zhang S, et al. Progress in methods for evaluating Schwann cell myelination and axonal growth in peripheral nerve regeneration via scaffolds. Front Bioeng Biotechnol. 2023;11:1308761. https://doi.org/10.3389/fbioe.2023.1308761.
41. Song J, Meng H, Deng G, et al. Sustainable release selenium laden with SiO(2) restoring peripheral nerve injury via modulating PI3K/AKT pathway signaling pathway. Int J Nanomed. 2024;19:7851–70. https://doi.org/10.2147/IJN.S460397.
42. Liu B, Xin W, Tan JR, et al. Myelin sheath structure and regeneration in peripheral nerve injury repair. Proc Natl Acad Sci U S Oct. 2019;29(44):22347–52. https://doi.org/10.1073/pnas.1910292116.
43. Sun J, Liao Z, Li Z, et al. Down-regulation miR-146a-5p in Schwann cell-derived exosomes induced macrophage M1 polarization by impairing the Inhibition on TRAF6/NF-kappaB pathway after peripheral nerve injury. Exp Neurol Apr. 2023;362:114295. https://doi.org/10.1016/j.expneurol.2022.114295.
44. Kamble N, Shukla D, Bhat D. Peripheral nerve injuries: electrophysiology for the neurosurgeon. Neurol India Nov-Dec. 2019;67(6):1419–22. https://doi.org/10.4103/0028-3886.273626.
45. Ciuffreda G, Bueno-Gracia E, Albarova-Corral I, et al. In vivo effects of joint movement on nerve mechanical properties assessed with Shear-Wave elastography: A systematic review and Meta-Analysis. Diagnostics (Basel). Feb. 2024;5(3). https://doi.org/10.3390/diagnostics14030343.
46. Ellefsen KL, Holt JR, Chang AC, et al. Myosin-II mediated traction forces evoke localized Piezo1-dependent Ca(2+) flickers. Commun Biol. 2019;2:298. https://doi.org/10.1038/s42003-019-0514-3.
47. Itson-Zoske B, Gani U, Mikesell A, et al. Selective RNAi-silencing of Schwann cell Piezo1 alleviates mechanical hypersensitization following peripheral nerve injury. Res Sq Oct. 2023;16. https://doi.org/10.21203/rs.3.rs-3405016/v1.
48. Zheng Q, Liu H, Yu W, et al. Mechanical properties of the brain: focus on the essential role of Piezo1-mediated mechanotransduction in the CNS. Brain Behav Sep. 2023;13(9):e3136. https://doi.org/10.1002/brb3.3136.
49. Shin SM, Itson-Zoske B, Fan F, et al. Peripheral sensory neurons and non-neuronal cells express functional Piezo1 channels. Mol Pain Jan-Dec. 2023;19:17448069231174315. https://doi.org/10.1177/17448069231174315.
50. Song Y, Li D, Farrelly O, et al. The mechanosensitive ion channel piezo inhibits axon regeneration. Neuron Apr. 2019;17(2):373–89. https://doi.org/10.1016/j.neuron.2019.01.050. e6.
51. Zuela-Sopilniak N, Lammerding J. Can't handle the stress? Mechanobiology and disease. Trends Mol Med Sep. 2022;28(9):710–25. https://doi.org/10.1016/j.molmed.2022.05.010.
52. Wu W, Xie J, Liu T, et al. Analysis of Biomechanical characterization of the thumb rubbing method. Technol Health Care. 2023;31(S1):505–13. https://doi.org/10.3233/THC-236044.
53. Gnanasambandam R, Ghatak C, Yasmann A, et al. GsMTx4: mechanism of inhibiting mechanosensitive ion channels. Biophys J Jan. 2017;10(1):31–45. https://doi.org/10.1016/j.bpj.2016.11.013.
54. Moya IM, Halder G. Hippo-YAP/TAZ signalling in organ regeneration and regenerative medicine. Nat Rev Mol Cell Biol Apr. 2019;20(4):211–26. https://doi.org/10.1038/s41580-018-0086-y.
55. Li HX, Zhang ZC, Peng J. Low-intensity extracorporeal shock wave therapy promotes recovery of sciatic nerve injury and the role of mechanical sensitive YAP/TAZ signaling pathway for nerve regeneration. Chin Med J (Engl). Oct 14. 2021;134(22):2710–2720. https://doi.org/10.1097/CM9.0000000000001431
56. Urbanski MM, Kingsbury L, Moussouros D, et al. Myelinating glia differentiation is regulated by extracellular matrix elasticity. Sci Rep Sep 20. 2016;6:33751. https://doi.org/10.1038/srep33751.
57. Grove M, Kim H, Santerre M, et al. YAP/TAZ initiate and maintain Schwann cell myelination. Elife Jan. 2017;26(6). https://doi.org/10.7554/eLife.20982.
58. Mindos T, Dun XP, North K, et al. Merlin controls the repair capacity of Schwann cells after injury by regulating Hippo/YAP activity. J Cell Biol Feb. 2017;216(2):495–510. https://doi.org/10.1083/jcb.201606052.
59. Pathak MM, Nourse JL, Tran T, et al. Stretch-activated ion channel Piezo1 directs lineage choice in human neural stem cells. Proc Natl Acad Sci U S Nov. 2014;11(45):16148–53. https://doi.org/10.1073/pnas.1409802111.

Publisher's note